

# Deformable MEMS grating for wide tunability and high operating speed

Maurizio Tormen<sup>1</sup>, Yves-Alain Peter<sup>2</sup>, Philippe Niedermann<sup>1</sup>, Arno Hoogerwerf<sup>1</sup> and Ross Stanley<sup>1</sup>

<sup>1</sup> Centre Suisse d'Electronique et de Microtechnique SA, Rue Jaquet-Droz 1, 2007 Neuchâtel, Switzerland

<sup>2</sup> Département de Génie Physique, Ecole Polytechnique de Montréal, Montréal, Canada

E-mail: [maurizio.tormen@csem.ch](mailto:maurizio.tormen@csem.ch)

Received 28 September 2005, accepted for publication 21 December 2005

Published 31 May 2006

Online at [stacks.iop.org/JOptA/8/S337](http://stacks.iop.org/JOptA/8/S337)

## Abstract

In optical MEMS, the family of diffractive MEMS is interesting for a wide range of applications, such as displays, scanners or switching elements. Their advantages are compactness, potentially high actuation speed and the ability to deflect light at large angles. A deformable diffraction MEMS grating is presented. Electrostatic actuation has experimentally proven a periodicity tuning of 2.5%. The device first resonant mode is expected to be at 28.5 kHz. The present device has been designed as a tuning element in an external cavity mid-infrared quantum-cascade laser.

**Keywords:** MEMS grating, tunable laser

(Some figures in this article are in colour only in the electronic version)

## 1. Introduction

In optical MEMS, the family of diffractive MEMS is interesting for a wide range of applications where more standard optical MEMS, in particular tilting mirrors [1–3], are currently used.

The advantages of diffractive MEMS are compactness, potentially high actuation speeds, the ability to deflect light at large angle and dynamically filtering light with narrow spectral responses.

Different application fields are currently looking at diffractive MEMS [1], such as information technology (e.g. projection displays, barcode readers, retina scanning readers), medicine (e.g. endoscopes), telecommunications (e.g. optical switch, wavelength tuning, variable optical attenuator), metrology (e.g. 3D shape measuring, spectroscopy), lithography (e.g. programmable masks) and astronomy (e.g. wavefront correction).

Commercially available diffractive MEMS devices are used in displays, in spectroscopy and in optical telecommunications [4, 5].

This paper presents a diffraction MEMS grating whose period can be modified through mechanical stretching. This device is conceived as tuning element for external cavity

lasers [6], in particular an external cavity mid-infrared (5  $\mu\text{m}$ ) quantum-cascade laser.

Electrostatic actuation has experimentally reached a periodicity tuning of 2.5%. This result is superior to the current state of the art [7–9]. In addition, the device can be operated at high frequencies, since its first resonant mode is expected at 28.5 kHz.

## 2. Design

Figure 1 shows the design of the deformable MEMS grating. The optical grating is formed by silicon beams etched in the device layer of an SOI wafer. The grating is designed with a duty-cycle of 50% and different periods,  $\Lambda$  (6, 9 and 12  $\mu\text{m}$ ). The grating beams, connected one to the other through grating springs, form a structure that is suspended through flexible beams and anchored to the substrate via the oxide layer at six different points. The grating springs act as leaf springs (figure 2): during actuation these are the only elements where stress is concentrated and, thus, where deformation is present. Moreover, they do not allow torsional movement to the grating beams around their longitudinal axes. The grating is stretched by two comb actuators.

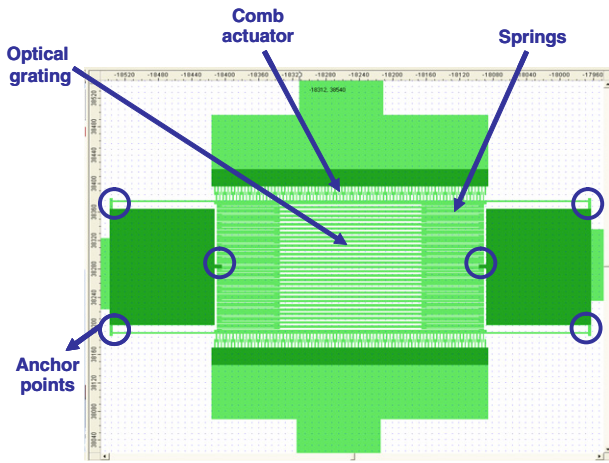


**Figure 1.** Overview of the deformable MEMS grating structure: it is possible to distinguish the beams forming the grating, the six anchor points at which the suspended structure is fixed and the comb actuators on both grating sides. The grating dimensions are on the order of  $200\ \mu\text{m} \times 200\ \mu\text{m}$ .

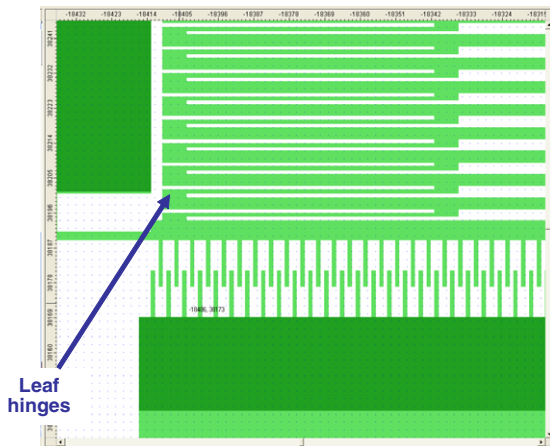


**Figure 2.** Detail of the deformable MEMS grating, in particular of the leaf hinge structures. The leaf hinges are formed by a thin flexible beam with two wide structures at its extremities: this structure provides the required spring constant without inducing any stress on the adjacent beams acting.

The mechanical properties of the structure were studied through finite element modelling. Commercial software (CoventorWare) was used to simulate the in-plane movement and the resonant modes of the structure, for which a non-adaptive Manhattan meshing, creating bricks as basic units, was chosen. Preliminary convergence tests were made to reduce simulation time. A maximum acceptable deviation from asymptotic results was fixed at 1%. In this way, the Manhattan meshing could be set to  $5\ \mu\text{m}$  along the three axes and the number of iterations for the electro-mechanical solver to one. This choice led to simulation times on the order of 10 min for each operating condition.

The first resonant mode is predicted to be at 28.5 kHz and is an in-plane mode, while the second and third modes are out-of-plane modes, expected at 60 and 68.5 kHz, respectively. These modes are at quite high frequencies given the size of

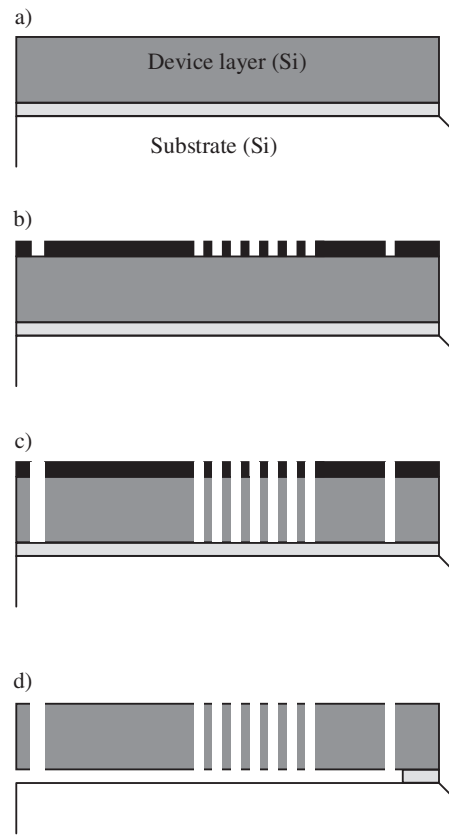


**Figure 3.** Process flow for the deformable MEMS grating fabrication. The SOI wafer has a  $10\ \mu\text{m}$  thick device layer and  $2\ \mu\text{m}$  thick bottom oxide. The photolithographic and etch steps define the grating beams, the springs and the comb actuators at the same time. The minimum feature is  $1\ \mu\text{m}$  wide. The HF vapour release step liberates the suspended elements: the grating beams, the springs and the comb actuators. (a) Start with a low-resistivity SOI wafer. (b) Patterning of structures. Minimum feature is  $1\ \mu\text{m}$ . (c) Dry etching of the device layer. The required etch is  $10\ \mu\text{m}$  deep. (d) Sacrificial oxide removal in HF vapour.

the structure and are due to the thickness of the device layer ( $10\ \mu\text{m}$ ).

The design requires only one mask level for the definition of the grating, the springs and the actuators.

### 3. Fabrication

Figure 3 shows the process flow. The process starts with a low resistivity SOI (silicon on insulator) wafer. The bottom oxide is  $2\ \mu\text{m}$  thick, while the device layer thickness is  $10\ \mu\text{m}$ : this choice guarantees sufficient stiffness to the wide suspended structure in order not to buckle and not to stick onto the substrate during the final release step. Photolithography defines structures with minimum feature as small as  $1\ \mu\text{m}$  and it is followed by dry reactive ion etching to define in a single step grating beams, springs and comb actuators. A good control of these steps is required in order to guarantee that all flexible structures have the same spring constant. The accuracy of the positioning of each grating beam depends on such a control.

The device is then released by removing the sacrificial oxide in HF vapour.

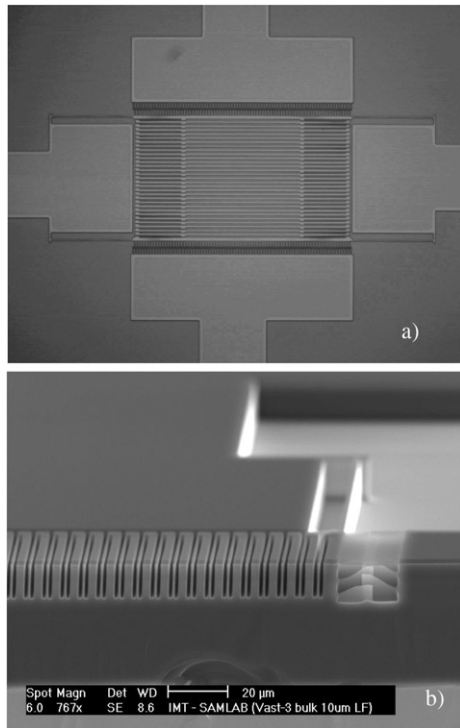


**Figure 4.** Devices fabricated on a Si test wafer. (a) Top view of an entire device (optical microscope). (b) Cross-section SEM image of the spring region for one test structure with  $6\ \mu\text{m}$  period. The high quality of the etching step guarantees an excellent reproducibility of the spring constant for the different grating springs.

A final coating step can be added (e.g. a gold coating) to give the required reflection properties for any specific spectral region.

Gratings with periods of  $6$ ,  $9$  and  $12\ \mu\text{m}$  were fabricated. Figures 4(a) and (b) show the top view of an entire device and a cross-section of the spring region, respectively, for a device with  $6\ \mu\text{m}$  period on a silicon test wafer.

#### 4. Mechanical characterization

The deformable gratings were tested by applying up to  $100\ \text{V}$  to the comb actuators. Figure 5 shows a detailed view of the grating (a) with no applied voltage and (b) with  $100\ \text{V}$  applied. In the latter case each end of the grating moves by  $2\ \mu\text{m}$ , resulting in an overall stretching of the structure of  $4\ \mu\text{m}$ . This is equivalent to a relative tuning of the grating period  $\Delta\Lambda/\Lambda$  of approximately  $2.5\%$ . This would correspond to a tuning range of  $120\ \text{nm}$  at the wavelength of interest,  $5\ \mu\text{m}$ .

In this measurement, maximum displacement is limited by the high voltage supply: in principle, the present structure can have a relative tuning  $\Delta\Lambda/\Lambda$  up to  $10\%$ .

Figure 6 shows the measured displacement of the comb actuator versus the applied voltage. Good agreement is obtained with the finite element simulations. The experimental deviation from the ideal quadratic behaviour (experimentally a linear behaviour of the displacement is found at higher voltages) is related to the mechanical properties of the flexible beams on which the structure is suspended (figure 1). In fact, the flexible beams cannot rotate freely around the axis

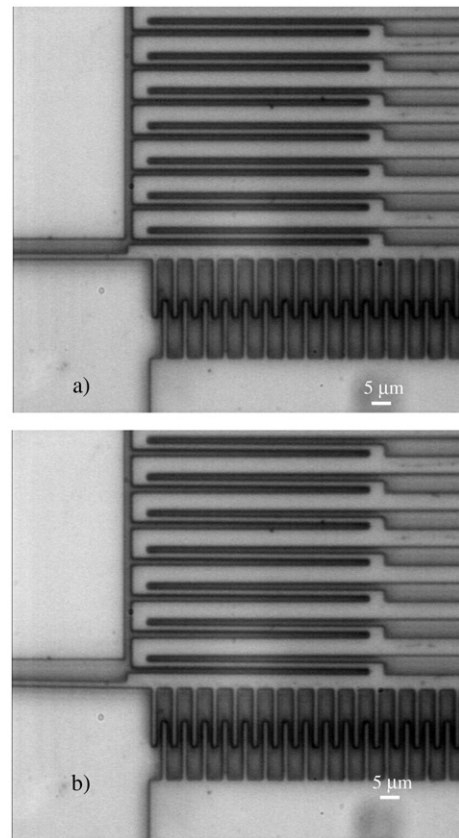


**Figure 5.** Top view of the electrostatic comb drive and spring region for two different actuation voltages: (a) no applied voltage; (b)  $100\ \text{V}$  applied. The displacement of the end of the grating is  $2\ \mu\text{m}$ .

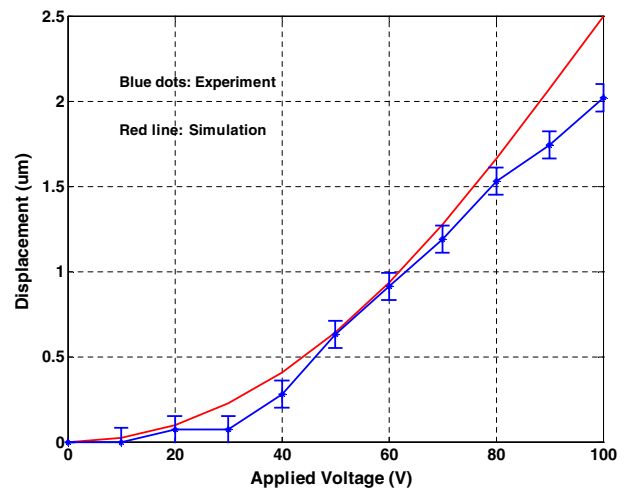


**Figure 6.** Measured and simulated displacement versus applied voltage for the  $12\ \mu\text{m}$  period grating. The maximum displacement at each grating end is  $2\ \mu\text{m}$ . A deviation from ideal quadratic behaviour (experimentally a linear behaviour of the displacement is found at higher voltages) is related to the design of the anchor points.

perpendicular to the suspended structure plane and passing through the anchor point itself. This mechanical constraint can be removed with a different design of the anchor point, enabling the full exploitation of the applied voltage.

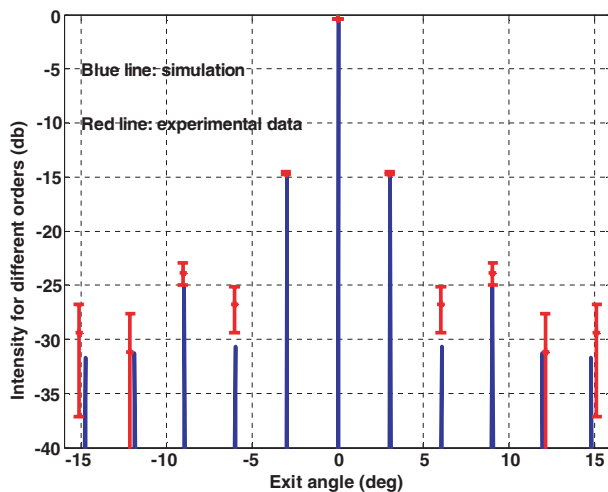


**Figure 7.** Optical characterization of the 12  $\mu\text{m}$  period grating with an He–Ne laser at 632.8 nm.

## 5. Optical characterization

The fabricated structures were tested optically with a He–Ne laser (632.8 nm) in a static condition.

Figure 7 presents experimental results for a grating with period 12  $\mu\text{m}$ . Good agreement is found between the experimental results and the optical simulations in which the geometrical parameters of the grating are derived from direct measurement: in particular, the grating duty cycle is 0.45 (figure 7).

In order use such an approach to tune mid-IR (5  $\mu\text{m}$ ) external cavity quantum-cascade lasers, the grating beams will be blazed in order to improve diffraction efficiency.

This device is better than the current state of the art in terms of the combination of maximum tuning range and actuation speed.

In fact high actuation speed can be obtained through a piezoelectric actuation mechanism [8, 9], but in this case a small tuning range is obtained (relative tuning  $\Delta\Lambda/\Lambda$  of 0.2% was achieved). On the other hand, if a thermal actuation mechanism is used [7], a wider tuning range can be achieved, but the actuation speed cannot be higher than some hundreds of hertz.

Finally, the surface quality that can be obtained with this approach is superior if compared to side etching approach and the proposed single-mask design is ideally suited for mid-IR applications, because of the required minimum features.

Good agreement is obtained between experiments and optical simulations using data derived from mechanical characterization (figure 8).

## 6. Conclusion

A deformable MEMS grating was designed, fabricated and mechanically and optically tested. Good agreement

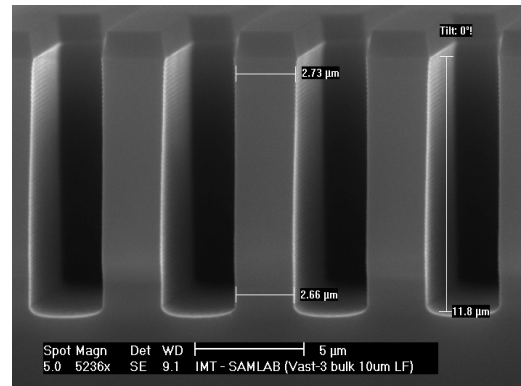


**Figure 8.** Cross-section SEM image of the grating beams in a test wafer.

between experimental results and expected performances was obtained.

If compared to the state of the art, this device extends both the tuning range and the operational frequency range of existing MEMS diffraction gratings.

The device will be used, in its blazed version, as a tunable element in mid-IR (5  $\mu\text{m}$ ) external cavity quantum-cascade (QC) lasers.

## Acknowledgments

This work was partly funded by the Swiss NCCR Quantum Photonics programme. We thank them for their support. We thank Dr Simon Henein for fruitful discussions on the spring design. The devices were fabricated in the clean rooms of COMLAB, the shared facilities of the Institute of Microtechnology, University of Neuchatel, and CSEM.

## References

- [1] Schenk H *et al* 2004 Photonic microsystems: an enabling technology for light deflection and modulation *Proc. SPIE* **5348** 7–21
- [2] Van Kessel P F *et al* 1998 A MEMS-based projection display *Proc. IEEE* **86** 1687–704
- [3] Dürr P *et al* 1999 Micromirror spatial light modulators *Proc. MOEMS '99* pp 60–5
- [4] [www.siliconlight.com](http://www.siliconlight.com)
- [5] [www.polychromix.com/html/products.htm](http://www.polychromix.com/html/products.htm)
- [6] Anthon D *et al* 2002 External cavity diode lasers tuned with silicon MEMS *OFC 2002 (March 2002)* pp 97–8
- [7] Zhang X M and Liu A Q 2000 A MEMS pitch-tunable grating add/drop multiplexers *Optical MEMS 2000 (August 2000)* pp 25–6
- [8] Chee W *et al* 2003 Analog tunable gratings driven by thin-film piezoelectric microelectromechanical actuators *Appl. Opt.* **42** 621–6
- [9] Chee W *et al* 2004 Analog piezoelectric-driven tunable gratings with nanometer resolution *J. Microelectromech. Syst.* **13** 998–1005